RevMexAA (Serie de Conferencias), **3**, 89–92 (1995)

3-D MODELS OF EMISSION FROM LOP-SIDED BOWSHOCKS

W. J. Henney
Instituto de Astronomía, UNAM, Apdo. Postal 70-264, 04510 México D.F., México

RESUMEN

Se calculan modelos analíticos estacionarios sencillos de choques de proa asimétricos. Se presentan imágenes monocromáticas para líneas en emisión tanto de alta como de baja excitación. Se encuentra que, cuando la asimetría del choque de proa se debe a un gradiente de densidad en el medio ambiente, las líneas de baja excitación son mas brillantes por el lado de alta densidad, mientras las líneas de alta excitación son más brillantes por el lado de baja densidad. Se ve exactamente el mismo comportamiento en Herbig-Haro 1, lo cual sugiere que, en este objeto, la asimetría está ocasionada por un gradiente sistemático de densidad del gas en frente del choque y no por efectos dinámicos no estacionarios.

ABSTRACT

Simple analytic steady-state models of asymmetrical bowshocks are calculated. Monochromatic images are presented for both high and low excitation emission lines. It is found that when the bowshock asymmetry is due to a density gradient in the ambient medium, then low excitation lines are brighter from the high density side, whereas high excitation lines are brighter from the low density side. Exactly this behavior is seen in Herbig-Haro 1, suggesting that, in this object, the asymmetry is caused by a systematic density gradient in the gas in front of the bowshock, rather than by time-dependent dynamic effects.

Key words: **HYDRODYNAMICS — ISM: INDIVIDUAL OBJECTS: HH 1 — ISM: JETS AND OUTFLOWS — LINE: PROFILES**

1. INTRODUCTION

Bowshocks are formed where jets from young stars interact with the ambient gas. Many Herbig-Haro objects, which have been interpreted as bowshocks, show pronounced asymmetry with respect to the jet axis (e.g., HH 1, HH 34). In the case of HH 1, this asymmetry has persisted for at least 50 years (Herbig & Jones 1981). Two possible classes of explanation for this asymmetry are (i) time-dependent dynamic effects, e.g., thermal instabilities (Raga et al. 1988), or precessing or "wiggly" jets (Biro & Raga 1994), or (ii) systematic asymmetries in the ambient medium of the jet. Here I investigate the feasibility and consequences of the second of these classes of explanation.

2. BOWSHOCK MODEL

I construct steady-state models of the bowshock, assuming balance between the pressure of the shocked jet gas and the ram pressure of the ambient gas entering the bowshock. Two possible sources of the bowshock asymmetry are considered:

1. Density gradient in the ambient medium.
2. Non-axisymmetric distribution of pressure in the shocked jet gas.

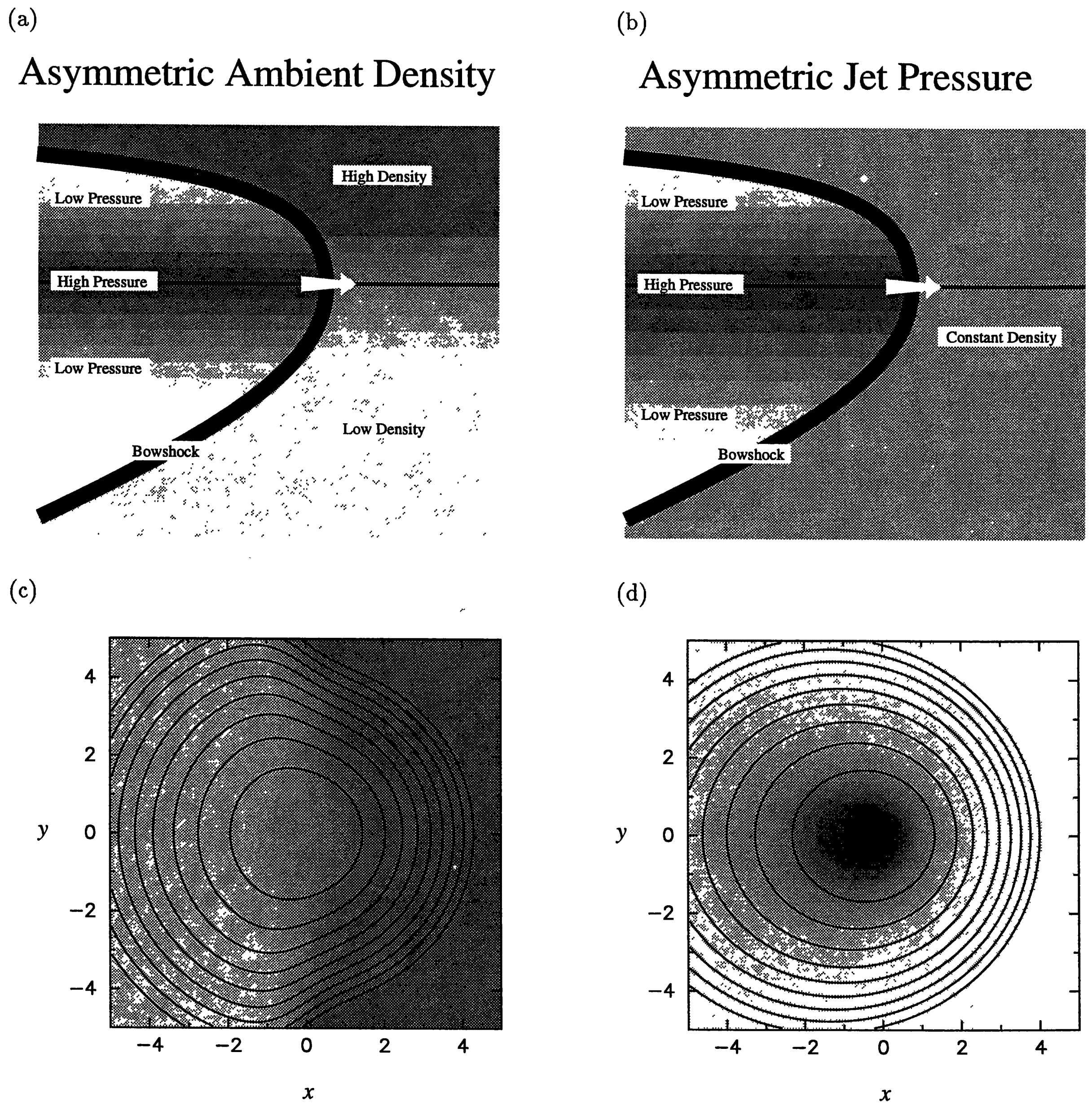

Fig. 1. A steady-state asymmetric bowshock may be caused (a) by a density gradient in the ambient medium or (b) by a non-axisymmetric pressure distribution in the shocked jet. Cross sections through the bowshock (i.e., cuts perpendicular to the jet axis) for these two scenarios are illustrated by contours in (c) and (d). Grey scales show the ambient density distribution in (c) and the jet pressure distribution in (d).

These are illustrated schematically in Figures 1a and b. A further possibility (not considered here) is a non-constant velocity field in the ambient gas.

Rather than attempt to calculate the bowshock shape from a given density and pressure distribution, I choose a shape for the bowshock and then infer the ambient density distribution (assuming axisymmetric jet pressure) for Case 1, or infer the jet pressure (assuming constant ambient density) for Case 2. In Case 1, an attempt is made to derive an ambient density distribution that is close to plane-parallel. Figures 1c and d show the bowshock cross-sections and density/pressure distributions for the two cases.

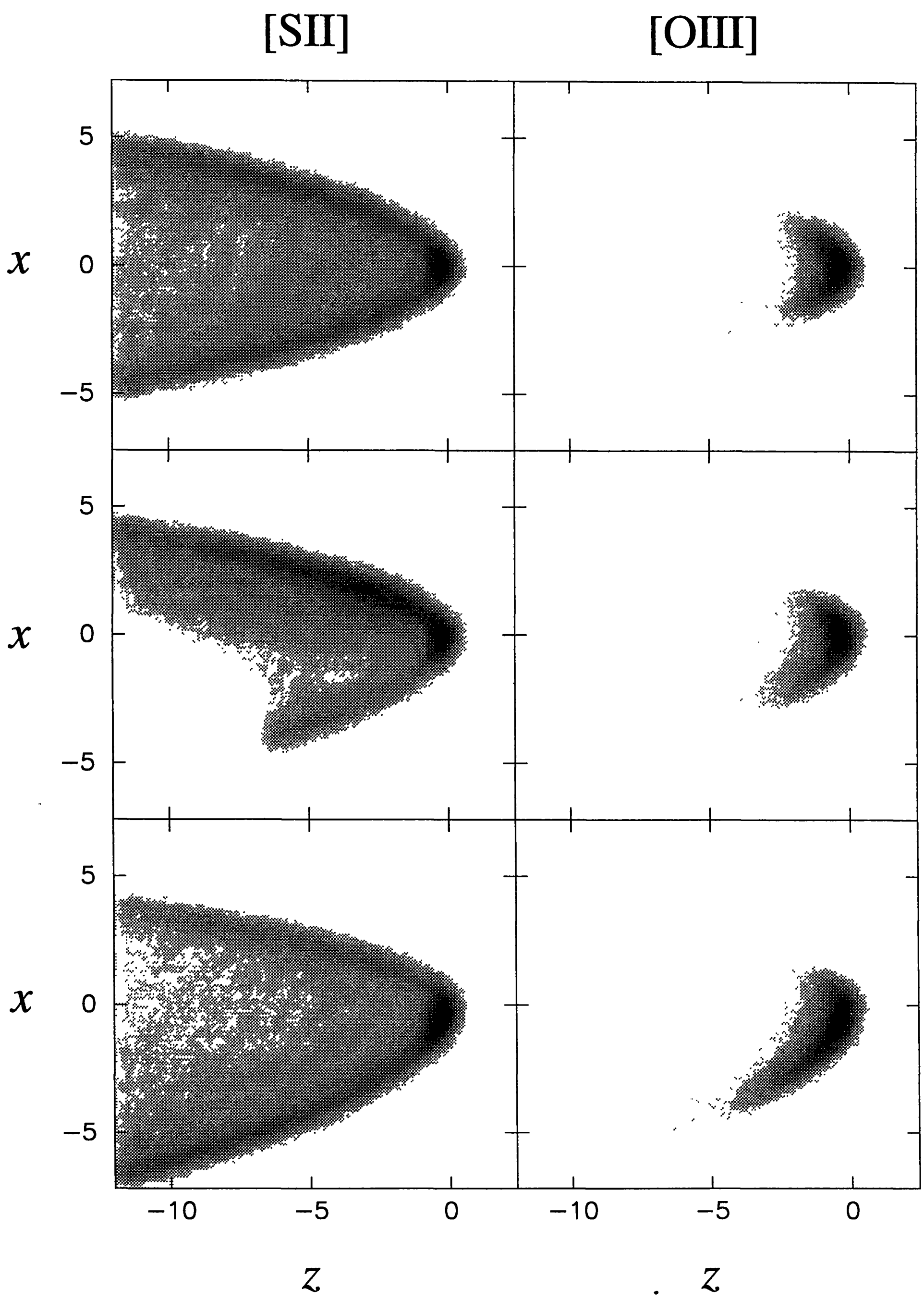

Fig. 2. Emission line images of bowshocks moving in the plane of the sky, showing the distinction between asymmetry in the ambient medium and in the jet pressure. Left column shows [S II], right column shows [O III]. See text for details.

2.1. Model Geometry

The jet is assumed to propagate along the z-axis, which is inclined by an angle α with respect to the plane of the sky. The density gradient or pressure skewness is directed along the x-axis, which is rotated by an angle β about the jet axis from the plane of the sky.

3. EMISSION LINE IMAGES

Emission lines are calculated using a "patchwork" of planar radiative shock models (Hartigan, Raymond, & Hartmann 1987). Resultant images are shown in Figure 2. All models have a bowshock velocity of 150 km s^{-1} and have $\alpha = \beta = 0$. The left-hand panels show emission from typical "low excitation" lines ([S II] 6716+6731), while the right-hand panels show typical "high excitation" lines ([O III] 4959+5007). The top pair of images show a symmetrical bowshock. The [O III] emission requires high post-shock temperatures and so only comes from the head of the bowshock. The [S II] lines on the other hand are emitted from a much more extended region.

The center two panels show a model with non-uniform ambient density. The density in the top half of the image is 3.4 times that in the bottom half. The [S II] emission is strongest from the side with the higher ambient density, whereas the [O III] emission, due to its strong dependence on the shock velocity, is strongest from the low density side, since the bowshock is more "open" to that side.

The bottom two panels show a model with a non-axisymmetric jet pressure. In this model, both the high and low excitation lines are stronger from the side towards which the pressure is skewed. Note that the [O III] emission is the more asymmetric, unlike in the previous model, because of its greater sensitivity to the shock velocity.

4. COMPARISON WITH OBSERVATIONS

Comparison of Hα and [O III] emission line images of the HH 1 bowshock (Raga et al. 1988) with the center panels of Figure 2 reveals a striking resemblance (the appearance of the models in Hα is very similar to that in [S II]). In particular, the observations show that the high excitation emission is skewed towards the opposite side of the jet axis from the low excitation emission, exactly as predicted by the model. This indicates that a large degree of the asymmetry seen in HH 1 is probably due to a density gradient in the gas in front of the bowshock, a conclusion that is further supported by the distribution of dust-scattered light upstream of the shock (Solf & Böhm 1991) and the fact that molecular hydrogen emission is only seen in the North-Eastern wing (Noriega-Crespo & Garnavich 1994). Recent *HST* images (see the paper by Hester et al. 1995) basically confirm this picture, while revealing a wealth of further detail that the simple model presented here cannot attempt to capture.

Further details of the model, together with more extensive results (including predictions for spatially resolved line profiles and treatment of scattering by upstream dust) will be presented elsewhere. I would like to thank A. Raga and J. Arthur for their many useful comments about this work.

REFERENCES

Biro, S., & Raga, A. C. 1994, ApJ, 434, 221
Hartigan, P., Raymond, J. C., & Hartmann, L. 1987, ApJ, 316, 323
Herbig, G. H., & Jones, B. F. 1981, AJ, 86, 1232
Hester, J. et al., 1995, in preparation
Noriega-Crespo, A., & Garnavich, P. M. 1994, RevMexAA, 28, 173
Raga, A. C., Mateo, M., Böhm, K. H., & Solf, J. 1988, AJ, 95, 1783
Solf, J., & Böhm, K. H. 1991, ApJ, 375, 618